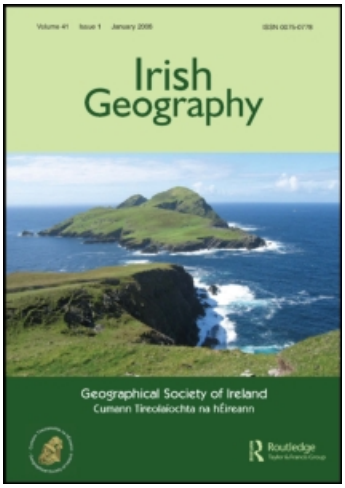

Irish Geography
Publication details, including instructions for authors and subscription information:
http://www.informaworld.com/smpp/title~content=t791546828

Statistical downscaling of temperature, radiation and potential evapotranspiration to produce a multiple GCM ensemble mean for a selection of sites in Ireland

Rowan Fealy [a]; John Sweeney [a]
[a] Department of Geography, NUI Maynooth, Co. Kildare, Ireland

To cite this Article Fealy, Rowan and Sweeney, John(2008) 'Statistical downscaling of temperature, radiation and potential evapotranspiration to produce a multiple GCM ensemble mean for a selection of sites in Ireland', Irish Geography, 41: 1, 1 — 27
To link to this Article: DOI: 10.1080/00750770801909235
URL: http://dx.doi.org/10.1080/00750770801909235

Irish Geography
Vol. 41, No. 1, March 2008, 1–27

Routledge
Taylor & Francis Group

Statistical downscaling of temperature, radiation and potential evapotranspiration to produce a multiple GCM ensemble mean for a selection of sites in Ireland

Rowan Fealy* and John Sweeney

Department of Geography, NUI Maynooth, Co. Kildare, Ireland

Irish climate is experiencing changes which have been found to be consistent with those occurring at a global scale. Consequently there is now growing confidence that these changes are largely attributable to global warming. Based on the data from four long-term monitoring, synoptic stations, between 1890 and 2004, mean annual temperatures in Ireland rose by 0.7°C. In the absence of strict emissions controls, a doubling of global atmospheric concentrations of CO_2 is likely by the end of the twenty-first century. As a consequence, global temperatures are projected to increase by between 1.8°C and 4°C over the same period depending on the climate sensitivity to increased levels of greenhouse gases. In order to determine the likely impact on Irish temperatures and related climatic variables, this paper illustrates a technique for downscaling Global Climate Model (GCM) output for a selection of sites in Ireland. Results of a weighted ensemble mean, derived from multiple GCMs, are presented in an attempt to address some of the various uncertainties inherent in climate modelling. Projected changes in selected indices of temperature extremes are also presented for a high emissions scenario (A2), as changes in extremes are likely to have a larger and more immediate impact on human society than changes in the mean climate state.

Keywords: statistical downscaling; Ireland; temperature; radiation; potential evapotranspiration

Introduction

Global average surface temperature has increased by 0.74°C over the last 100 years (IPCC 2007). While the global temperature record displays a large degree of variability, most of this warming occurred during two periods; 1910–1945 and 1979–2006. The rate of warming during the latter period of 1979–2006 has been faster over land than the oceans. In the Northern Hemisphere, the 1990s was the warmest decade and 1998 was the warmest year, since reliable global instrumental records began in 1861 (IPCC 2001, Jones and Moberg 2003). This was followed by the joint second warmest years of 2005 and 2003, followed by 2002 and 2004. Eleven of the 12 warmest years in the instrumental record have occurred between 1995 and 2006 with the twelfth warmest year occurring in 1990. Proxy records indicate that the temperature increases recorded during the twentieth century in the Northern Hemisphere resulted in it being the warmest century in the last millennium (IPCC 2001). Much of this warming has occurred in the winter, spring and autumn seasons

*Corresponding author. Email: rowan.fealy@nuim.ie

ISSN 0075-0778 print/ISSN 1939-4055 online

DOI: 10.1080/00750770801909235
http://www.informaworld.com

(Jones *et al*. 2001). There is also evidence to suggest that the rate of warming has accelerated in recent decades, with the warming rate of the past 50 years almost double that of the past 100 years (IPCC 2007).

Based on the data from four, long-term, synoptic stations (Valentia, Malin Head, Armagh and Birr), McElwain and Sweeney (2007) calculated a mean annual temperature anomaly for Ireland which displayed a linear increase of 0.7°C over the 1890–2004 period. This increase largely occurred over two periods, between 1910 to 1949 and 1980 to 2004, in line with global trends. However, the warmest year in Ireland remains 1945, with an anomaly of 1.18°C above the 1961–1990 period. However, preliminary figures released by Met Éireann for 2007 indicate that a number of stations around the country recorded their warmest year (Valentia Observatory, Malin Head, Belmullet, Rosslare and Kilkenny) and hence 2007 may replace 1945 as the warmest on record in the Irish temperature anomaly. For the period 1960 to 2000, increases in minimum temperatures were found to be greater than increases in maximum temperatures during the summer and autumn, while during the winter months, maximum temperatures increased more (Sweeney *et al.* 2002). Similar to global trends, winter warming is contributing a greater proportion to the increases in annual temperature. However, increasing winter temperatures in Ireland are being driven by changes in maximum temperatures and not minimum temperatures, in contrast to the global trend.

Trends in the Irish temperature records have been found to be largely consistent with those occurring at a global scale (McElwain and Sweeney 2007). There is now increased confidence that these global changes are largely attributable to the observed increase in anthropogenic greenhouse gas concentrations (IPCC 2001). In the absence of strict emissions controls with a consequent increase in atmospheric concentrations of greenhouse gases, Global Climate Models (GCMs) project an increase in global temperatures of 1.8–4.0°C over the course of the present century (Figure 1) (IPCC 2007). An increase of this magnitude is likely to have a significant impact on climate processes operating from global and hemispherical scales, to the regional and local-scale surface environmental variables.

Despite the high degree of sophistication of GCMs, their output is generally too coarse to be useful for regional or local-scale impacts analysis, as important processes which occur at sub-grid scale are not, at present, resolved by these models (Wilby *et al.* 1999). Changes in both temporal and spatial variability, which may be just as important as the magnitude of change, are also masked at the sub-grid scale (Wigley *et al.* 1990), as it is unlikely that all locations will warm by the same amount and at the same rate. Global variations in the amount and rate of warming will also affect the distribution and rates of change of other meteorological variables, such as precipitation, radiation receipts and potential evapotranspiration (PE). Therefore a discrepancy in scale exists between the global scenarios, as output by GCMs, and changes that are likely to occur at the regional or local level due to these large-scale changes. In order to overcome some of these scale differences, a number of statistical downscaling techniques have been developed in which large-scale GCM output can be translated or 'downscaled' into information about changes in the climate which can then be used for local-scale impact analysis.

Empirical statistical downscaling is one such technique employed where high spatial and temporal resolution climate scenarios are required. The methodologies employed in statistical downscaling are largely common with those of synoptic

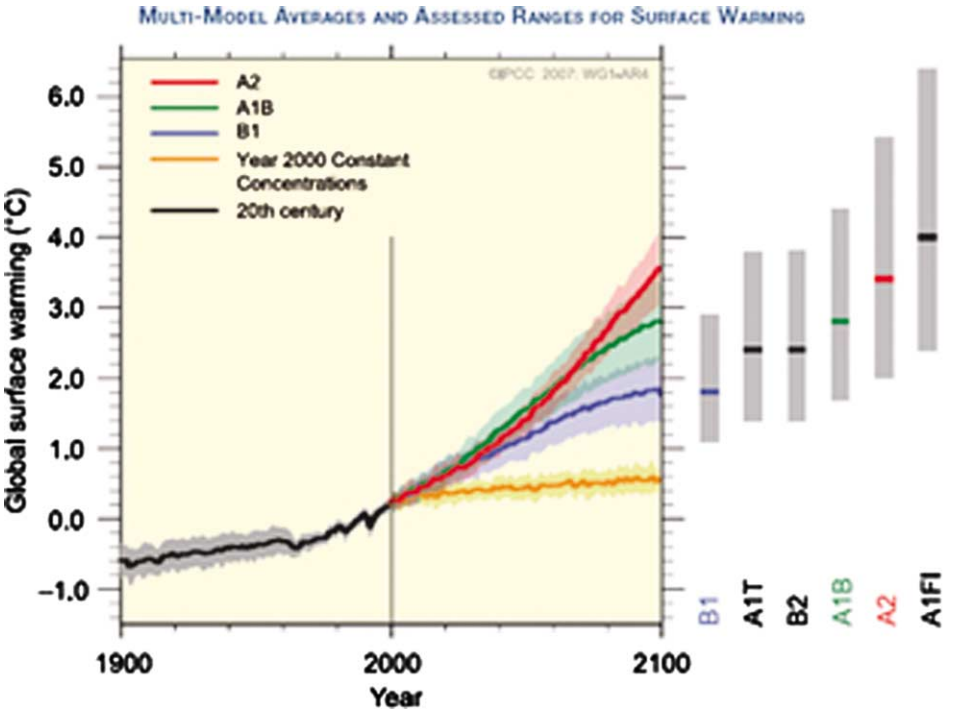

Figure 1. Projected global surface warming for the twenty-first century for six emissions scenarios. Source: IPCC, 2007.

climatology. However, the goal of downscaling is to adequately describe the relationship between atmospheric circulation and the surface environment, with attention being focused more on model parsimony and accuracy, rather than understanding the relationship between them (Yarnal *et al.* 2001). As a consequence of their relative ease of implementation and comparability of output to Regional Climate Models, the use of statistical downscaling methodologies to produce climate scenarios from GCMs is now widespread within the research community.

Statistical downscaling requires that a number of assumptions are made, the most fundamental of which is that the relationship established between predictor and predictand will remain constant under climate change conditions. This assumption has been found to be reliable under such conditions (Busuioc *et al.* 1998).

The selection of an optimum predictor set of atmospheric variables has been the focus of much research. However, no one technique or predictor set has come to the fore and there has been little research in evaluating the accuracy of various atmospheric predictor sets between studies and regions. Cross-comparisons between predictors and evaluation of skill has been complicated by the fact that different studies have utilised different techniques and atmospheric predictor combinations for different regions. A number of studies have shown that choice of technique (Wilby *et al.* 1998, Huth 2003) and predictors can have an impact on the resulting downscaled scenarios (Winkler *et al.* 1997, Huth 2003). Ultimately the number and choice of candidate predictors available for use is constrained by the overlap between

the National Centres for Environmental Prediction (NCEP) data and the output from the various modelling centres (Wilby and Dawson 2004).

The aim of this paper is to present a statistical downscaling methodology to downscale temperature, radiation and PE for Ireland. The downscaling methodology described is based on developing a regression equation that establishes a robust relationship between observed large-scale atmospheric predictors and an observed surface climate variable of interest for a particular location and season. Having calibrated and verified the linear relationship based on the observed data, comparable GCM model projected large-scale atmospheric predictors can then be employed to project the climate for a location and season. In order to account for uncertainties inherent in global climate modelling, a number of climate models and emissions scenarios are then employed to produce multi-model averages or ensembles of the downscaled modelled data.

Data

Data sources

Observed daily data for precipitation, maximum and minimum temperature and sun hours were obtained from 14 synoptic stations from the Irish meteorological service, Met Éireann, for the period 1961–2000. Potential evapotranspiration, based on the Penman-Montieth formula, was obtained for the 1971–2000 period, while radiation, obtained for the 1961–2000 period, was only available from a selection of synoptic stations. The synoptic stations represent low-lying conditions for a mixture of coastal and interior locations (Figure 2). Homogeneity analysis of the daily data was not performed as part of this research, primarily because the data obtained are from the synoptic network which are manned by experienced meteorological officers. Therefore the data are considered to be of good quality. With the exception of potential evapotranspiration, the data are provided with quality control flags, indicating whether a measurement is the value as read, accumulated, trace or otherwise, therefore enabling the researcher to decide on a suitable threshold for accepting the data as valid. In the present research, all values not directly measured by the observer were removed from the analysis, with the exception of potential evapotranspiration which is a calculated variable. Downscaled precipitation amounts and occurrences for each site, based on the suite of GCMs employed in this analysis, were obtained from Fealy and Sweeney (2007) as additional predictor variables for use in the downscaling methodology outlined below.

Large-scale surface and atmospheric data were obtained from the UKSDSM (United Kingdom Statistical DownScaling Model) data archive (Wilby and Dawson 2004) derived from NCEP Reanalysis data. The extracted variables were: daily grid point mean sea-level pressure, 500 hPa and 850 hPa geopotential heights, relative humidity from each of the geopotential heights, near surface specific humidity and mean temperature (Table 1). A number of important secondary variables were also extracted from the archive, based on a 3×3 grid domain centred over Ireland, according to the methods described by Jones *et al.* (1993). These secondary variables, which convey important information about the state and stability of the circulation, consisted of daily vorticity, zonal velocity component, meridional velocity component, geostrophic airflow velocity and divergence.

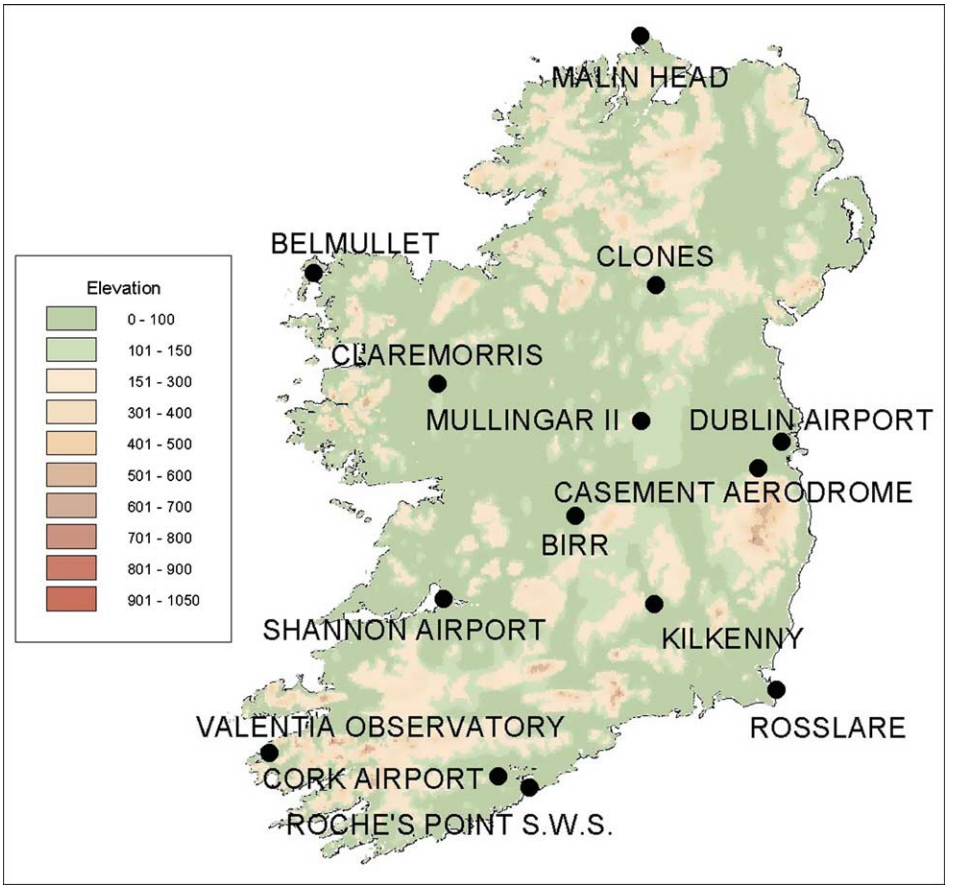

Figure 2. Location of synoptic stations employed in the analysis.

Table 1. List of primary candidate predictor variables for use in the analysis from the UKSDSM data archive.

Variable
Mean temperature
Mean sea level pressure
500 hPa geopotential height
850 hPa geopotential height
Near surface relative humidity
Relative humidity at 500 hPa height
Relative humidity at 850 hPa
Near surface specific humidity
Geostrophic airflow velocity
Vorticity
Zonal velocity component
Meridional velocity component
Divergence

Note: Italics indicate secondary airflow indices calculated from pressure fields (surface, 500 and 850 hPa).

In order to derive the future climate scenarios based on the described downscaling methodology, GCM data were obtained, again from the UKSDSM archive, for three models, namely the Hadley Centre (HadCM3), Canadian Centre for Climate Modelling and Analysis (CCCma) (CGCM2) and the Commonwealth Scientific and Industrial Research Organisation (CSIRO) (Mark 2), for both the A2 and B2 emissions scenarios (Wilby and Dawson 2004). All the gridded datasets exist on a common grid resolution, that of 2.5×3.75 degrees, and for a common grid domain. The lead and lag of each predictor was also calculated to allow for a temporal offset which may occur between the predictor and predictand.

Data calculations

As global solar radiation is only measured at a limited number of synoptic stations, sun hours, measured at all synoptic stations, was used in conjunction with the Angstrom formula in order to calculate radiation (Angstrom 1924, Brock 1981). The Angstrom formula calculates radiation from sun hours as follows

$$Q/Qa = a + b\left(\frac{n}{N}\right)$$

where Q is the received solar radiation (MJ m^{-2}),
Qa is the potential solar radiation at the top of the atmosphere (MJ m^{-2}),
n is sunshine (hours) and
N is the total day length

Values for the constants a and b (0.21 and 0.67 respectively) employed in the Angstrom formula were previously established for Ireland by McEntee (1980) and were found to provide a reasonably good approximation for global solar radiation in Ireland (Sweeney and Fealy 2003a) when applied to the Angstrom formula.

Methodology

For the present study, a stepwise multiple linear regression was employed in order to link the large-scale data to the predictands or surface climate variable of interest. This method is particularly suitable for use in downscaling studies where the predictand tends towards a normal or near normal distribution. Any predictand that conforms to this requirement can be adequately modelled using a standard multiple linear regression technique, as follows

$$Y = a + a_1x_1 + a_2x_2 + \ldots\ldots + a_nx_n + e$$

Y = predictand
a_n = coefficient
x_n = predictors
e = error term

The error term, e, can be employed to inflate the variance of the downscaled weather variables, which often tends to be underestimated, by adding 'white noise' to the predicted series.

Predictor selection

The candidate predictor data set, comprising of large-scale surface and atmospheric variables from the NCEP Reanalysis Project, was split into a calibration and verification period. The calibration period for temperature spanned 1961–1978 and 1994–2000, while the period 1979–1993 was withheld for verification purposes. The selection of these periods was arbitrary, but coincided with periods being employed by the STARDEX project (Statistical and Regional dynamical Downscaling of Extremes for European regions) to allow for comparison of results where possible. The calibration periods for radiation and PE differed from that of temperature. The calibration period for radiation was based on the 1971–2000 period, with 1961–1970 being withheld for verification to facilitate a comparison of modelled radiation, derived from sun hours, against actual measured radiation at a selection of sites. While potential evapotranspiration data was only available for the 1971–2000 period, the period 1991–2000 was withheld for independent verification.

In all, 53 candidate predictors were eligible for selection in the downscaling procedure. All potential predictors were assessed for suitability based on a number of criteria, such as significance and strength of correlation with individual predictands for each site and season. Predictors that demonstrated a degree of consistency across all sites were preferentially selected. Cross-correlations were also assessed between predictors in order to select a parsimonious data set with the aim of reducing issues associated with multicollinearity. Selected surface and atmospheric predictors were then used to calibrate the statistical transfer functions on a seasonal basis, linking the large-scale variables to the climate variable of interest, for each site and season. Tables 2 and 3 identify the most commonly selected predictors, for each season, for both maximum and minimum temperatures.

In addition to employing large-scale surface and atmospheric variables as predictors for downscaling temperature, local, site-specific surface variables were also employed in conjunction with the large-scale predictors for downscaling radiation and potential evapotranspiration. This modification to the more 'traditional' downscaling methodology is one that was adapted for the purposes of this research from conventional weather generator techniques, where local site-specific variables are employed as predictors in conjunction with the large-scale predictors in some form of a regression model as opposed to just employing the large-scale forcing provided from the reanalysis data. An important justification for the inclusion of

Table 2. Number of stations for which the most commonly occurring predictors were selected as inputs to calibrate the regression models for maximum temperature.

Season	Relative humidity	Zonal velocity component	Meridional velocity component	Geopotential height 500 hPa	Vorticity	Mean temperature
DJF	–	13 (ld)/1	11 (ld)/1	12 (ld)/1	2	13
JJA	–	1 (ld)/10	12	–	10 (ld) (850)/1	14
MAM	12	11 (850)	9 (ld)	–	12	14
SON	14 (l)	11 (500)	14 (ld) (850)	14	–	14 (l)

Notes: (l) indicates the lag of a variable, (ld) the lead of a variable. Number in brackets indicates the measurement level (hectopascals), where not specified, the measurements represent surface level. (DJF – Dec to Feb; MAM – Mar to May; JJA – Jun to Aug; SON – Sep to Nov)

Table 3. Number of stations for which the most commonly occurring predictors were selected as inputs to calibrate the regression models for minimum temperature.

Season	Geostrophic airflow velocity	Zonal velocity component 500 hPa	Geopotential height 500 hPa	Near surface relative humidity	Mean temperature (l)
DJF	12	–	13	–	14
JJA	14 (850)	8	10	14	14
MAM	13	1	14	14	14
SON	12	1	12	13	14

Notes: (l) indicates the lag of a variable, (ld) the lead of a variable. Number in brackets indicates the measurement level (hectopascals), where not specified the measurements represent surface level.

site-specific variables for downscaling radiation and potential evapotranspiration arises from their dependence on local conditions such as cloud cover: a process which occurs at sub-grid scale and therefore not well represented by the large-scale gridded data. Therefore, employing local climate variables as predictors, such as temperature range and precipitation which reflect thermal heating and local cloud cover, should provide additional and useful local-scale information. The inclusion of these additional variables was found to be justified in this research. For example, large-scale surface temperature from the NCEP reanalysis data was employed in combination with precipitation and temperature range (maximum–minimum temperature) from the relevant synoptic station as input to calibrate the seasonal radiation models at each site. Similarly for potential evapotranspiration, radiation, precipitation occurrence and precipitation amounts were used as inputs to calibrate the regression model. While wind plays an important role in the calculation of potential evapotranspiration, its importance has a seasonal dependence, being more influential during the winter months and diminishing during the spring, summer and autumn months. As calculated potential evapotranspiration values are at a minimum during the winter months, and based on previous research undertaken by the author (Sweeney and Fealy 2003a), the exclusion of this variable is unlikely to significantly impact the predicted values of potential evapotranspiration.

Results

Results of the calibration and verification period for maximum and minimum temperature, radiation and potential evapotranspiration are shown in Tables 4–7. A significant portion of the variance is accounted for in the seasonal regression models, particularly for the maximum and minimum temperature and potential evapotranspiration data, suggesting satisfactory modelling of the climate series in all seasons. Figures 3 and 4 illustrate the mean monthly observed and modelled data for maximum temperatures at Valentia, a coastal site, and Kilkenny, an inland site, for the verification period of 1979–1993. Figures 5 and 6 show the results of the modelled radiation derived from sun hours for the verification period 1961–1970 for Malin Head and Rosslare. Comparison of modelled radiation with actual radiation for the independent verification period indicate that monthly average totals have

Table 4. Pearson's r values for the seasonal calibration and verification periods for maximum temperatures.

Maximum temp. Stations	DJF		MAM		JJA		SON	
	Cal.	Ver.	Cal.	Ver.	Cal.	Ver.	Cal.	Ver.
Valentia Observatory	0.88	0.87	0.89	0.90	0.83	0.84	0.88	0.86
Shannon Airport	0.89	0.88	0.89	0.91	0.82	0.84	0.88	0.87
Dublin Airport	0.82	0.81	0.87	0.89	0.80	0.82	0.87	0.87
Malin Head	0.83	0.86	0.83	0.86	0.78	0.78	0.85	0.84
Roche's Point	0.89	0.88	0.85	0.87	0.76	0.80	0.86	0.87
Belmullet	0.85	0.86	0.85	0.87	0.79	0.79	0.86	0.85
Clones	0.86	0.85	0.87	0.90	0.81	0.82	0.87	0.86
Rosslare	0.90	0.90	0.86	0.86	0.74	0.79	0.87	0.87
Claremorris	0.87	0.86	0.87	0.90	0.79	0.82	0.86	0.86
Mullingar	0.88	0.88	0.87	0.91	0.80	0.85	0.87	0.87
Kilkenny	0.90	0.89	0.89	0.91	0.83	0.85	0.87	0.87
Casement Aerodrome	0.90	0.89	0.88	0.90	0.81	0.84	0.87	0.87
Cork Airport	0.90	0.89	0.87	0.89	0.80	0.84	0.87	0.87
Birr	0.89	0.88	0.89	0.92	0.83	0.85	0.87	0.87

been adequately captured by the technique employed, which uses a combination of large-scale and local predictors.

Figure 7 shows the comparison between observed radiation at Valentia and modelled radiation, calculated from the Angstrom formula employing sun hours, again for an independent verification period of 1961–1970. Slight underestimations in the modelled radiation values are apparent from the January to September period, due to the underestimation of radiation derived from the Angstrom formula and

Table 5. Pearson's r values for the seasonal calibration and verification periods for minimum temperatures.

Minimum temp. Stations	DJF		MAM		JJA		SON	
	Cal.	Ver.	Cal.	Ver.	Cal.	Ver.	Cal.	Ver.
Valentia Observatory	0.83	0.81	0.82	0.81	0.73	0.74	0.84	0.85
Shannon Airport	0.84	0.83	0.84	0.86	0.77	0.80	0.88	0.89
Dublin Airport	0.79	0.81	0.83	0.85	0.75	0.81	0.88	0.89
Malin Head	0.77	0.80	0.80	0.82	0.72	0.74	0.84	0.83
Roche's Point	0.85	0.84	0.88	0.89	0.82	0.85	0.90	0.90
Belmullet	0.81	0.80	0.81	0.82	0.70	0.72	0.81	0.81
Clones	0.78	0.79	0.82	0.83	0.74	0.77	0.86	0.86
Rosslare	0.81	0.82	0.86	0.88	0.81	0.84	0.89	0.89
Claremorris	0.81	0.80	0.82	0.83	0.73	0.75	0.85	0.86
Mullingar	0.79	0.78	0.83	0.82	0.75	0.76	0.87	0.87
Kilkenny	0.78	0.77	0.79	0.79	0.71	0.73	0.83	0.85
Casement Aerodrome	0.80	0.80	0.82	0.82	0.75	0.77	0.87	0.88
Cork Airport	0.85	0.85	0.87	0.88	0.83	0.84	0.91	0.91
Birr	0.82	0.82	0.84	0.82	0.74	0.77	0.87	0.88

Table 6. Pearson's r values for the seasonal calibration and verification periods for radiation.

Radiation Stations	DJF		MAM		JJA		SON	
	Cal.	Ver.	Cal.	Ver.	Cal.	Ver.	Cal.	Ver.
Valentia Observatory	0.66	0.67	0.73	0.66	0.62	0.58	0.73	0.72
Shannon Airport	0.65	0.62	0.77	0.65	0.68	0.62	0.74	0.71
Dublin Airport	0.61	0.62	0.69	0.68	0.60	0.54	0.73	0.73
Malin Head	0.70	0.69	0.67	0.66	0.47	0.46	0.73	0.74
Roche's Point	0.61	0.56	0.71	0.66	0.60	0.58	0.74	0.72
Belmullet	0.71	0.70	0.73	0.67	0.59	0.56	0.74	0.72
Clones	0.67	0.69	0.76	0.73	0.67	0.63	0.75	0.71
Rosslare	0.62	0.57	0.63	0.67	0.42	0.48	0.72	0.71
Claremorris	0.70	0.69	0.76	0.70	0.66	0.61	0.76	0.72
Mullingar	0.65		0.75		0.65		0.74	
Kilkenny	0.63	0.63	0.72	0.69	0.65	0.58	0.73	0.70
Casement Aerodrome	0.63	0.65	0.71	0.71	0.65	0.61	0.74	0.72
Cork Airport	0.63	0.62	0.75	0.85	0.67	0.64	0.77	0.77
Birr	0.66	0.63	0.75	0.67	0.67	0.61	0.74	0.72

used to calibrate the downscaling model. However, results are encouraging despite the fact that observed global solar radiation was not available for use in calibrating the regression models.

Figures 8 and 9 show the comparison between derived potential evapotranspiration at Valentia and Kilkenny and the modelled values of potential evapotranspiration from the statistical downscaling models. Again, the correspondence between monthly average totals for calculated and modelled potential evapotranspiration for the independent verification period suggests that the transfer functions and selected predictors are capable of reproducing statistics that are comparable with those of the

Table 7. Pearson's r values for the seasonal calibration and verification periods for potential evapotranspiration.

Potential evapotranspiration Stations	DJF		MAM		JJA		SON	
	Cal.	Ver.	Cal.	Ver.	Cal.	Ver.	Cal.	Ver.
Valentia Observatory	0.91	0.91	0.94	0.95	0.91	0.92	0.95	0.96
Shannon Airport	0.91	0.92	0.94	0.94	0.92	0.91	0.95	0.95
Dublin Airport	0.90	0.91	0.93	0.94	0.90	0.90	0.94	0.95
Malin Head	0.90	0.92	0.94	0.95	0.91	0.93	0.96	0.97
Belmullet	0.90	0.91	0.93	0.95	0.89	0.90	0.94	0.96
Clones	0.91	0.91	0.94	0.94	0.93	0.93	0.94	0.94
Rosslare	0.91	0.93	0.93	0.95	0.91	0.93	0.95	0.96
Mullingar	0.92	0.93	0.94	0.94	0.92	0.91	0.95	0.95
Kilkenny	0.90	0.92	0.92	0.93	0.91	0.92	0.94	0.95
Casement Aerodrome	0.89	0.92	0.93	0.93	0.90	0.91	0.93	0.94
Cork Airport	0.91	0.92	0.94	0.94	0.90	0.92	0.95	0.96
Birr	0.91	0.92	0.94	0.94	0.92	0.91	0.94	0.94

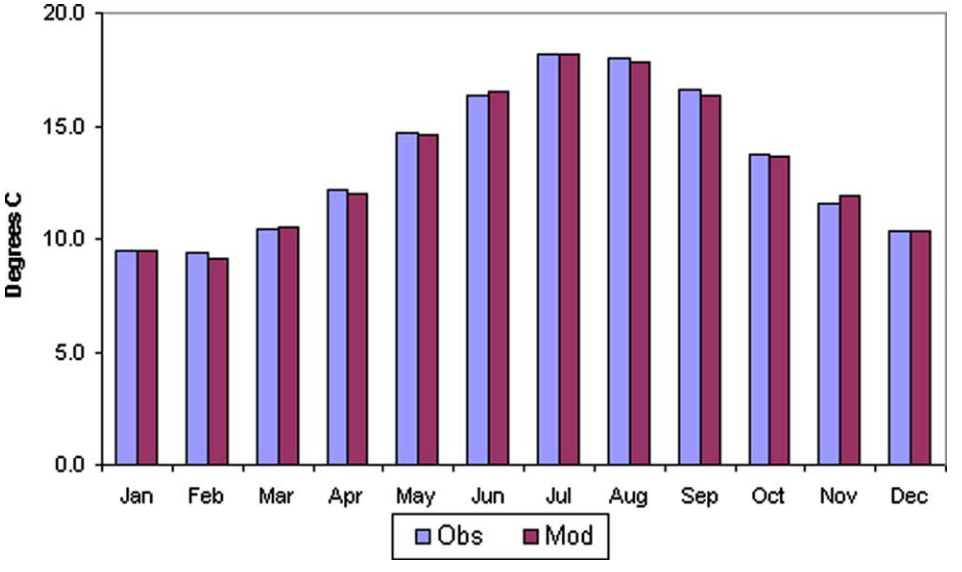

Figure 3. Comparison of observed and modelled maximum temperatures from Valentia, for the independent verification period 1979–1993.

observed data. While the model has a slight tendency to overestimate PE during June, July and August, the month-by-month results are encouraging.

Comparison of observed/calculated and modelled results for all variables, illustrated in both the Pearson's r values (Tables 4–7) and graphically (Figures 3–9), indicate that the technique employed, that of stepwise multiple linear regression, has adequately captured the seasonal forcing component of the large- and local-scale predictors employed and which explain a significant portion of variability in the observed variables of interest. Results for potential evapotranspiration display the highest Pearson's r values for the independent verification period, with all stations showing an r value greater than 0.8. Verification values for both maximum and minimum temperatures also display high r values, in excess of 0.7. Pearson's r values for radiation tended to be lower for both calibration and verification with values generally greater than 0.6, however, results for the summer (JJA) verification period tend to be weaker, with r values of between 0.4 and 0.6 apparent for this season.

Projected future changes in mean temperature, radiation and potential evapotranspiration in Ireland

In order to produce simulations of future changes in temperature, radiation and potential evapotranspiration as a consequence of climate change, data from the HadCM3, CSIRO and CCMA GCMs were employed as predictor variables in conjunction with the calibrated transfer functions, outlined in the methodology section, which linked the large-scale atmospheric data to the climate variables of interest. Although it has long being recognised that different GCMs produce significantly different regional climate responses even when forced with the same emissions scenario (Hulme and Carter 1999), it was common practice until recently for many impact studies to employ only one climate change scenario, based on one

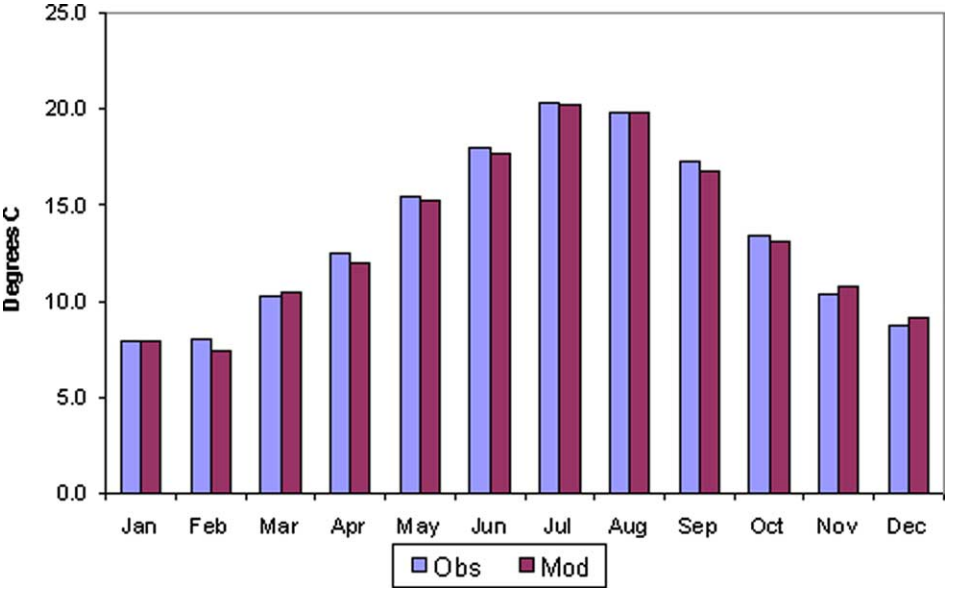

Figure 4. Comparison of observed and modelled maximum temperatures from Kilkenny, for the independent verification period 1979–1993.

emissions scenario, derived from a single GCM. Hulme and Carter (1999) consider this practice, which ultimately results in the suppression of crucial uncertainties, as 'dangerous' due to any subsequent policy decisions which may only reflect a partial assessment of the risk involved.

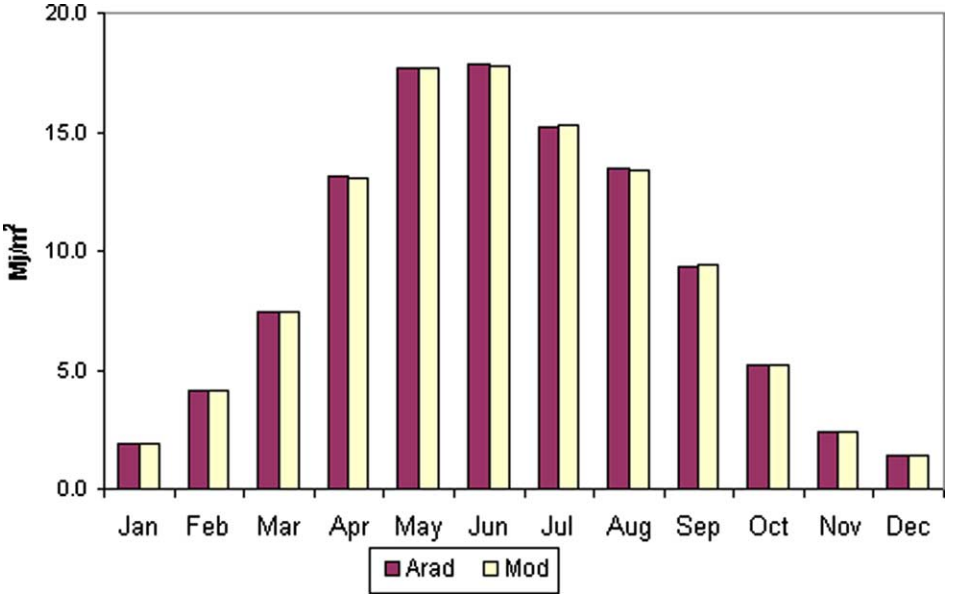

Figure 5. Comparison of mean daily radiation derived from sun hours from Malin Head and modelled radiation for an independent verification period of 1961–1970.

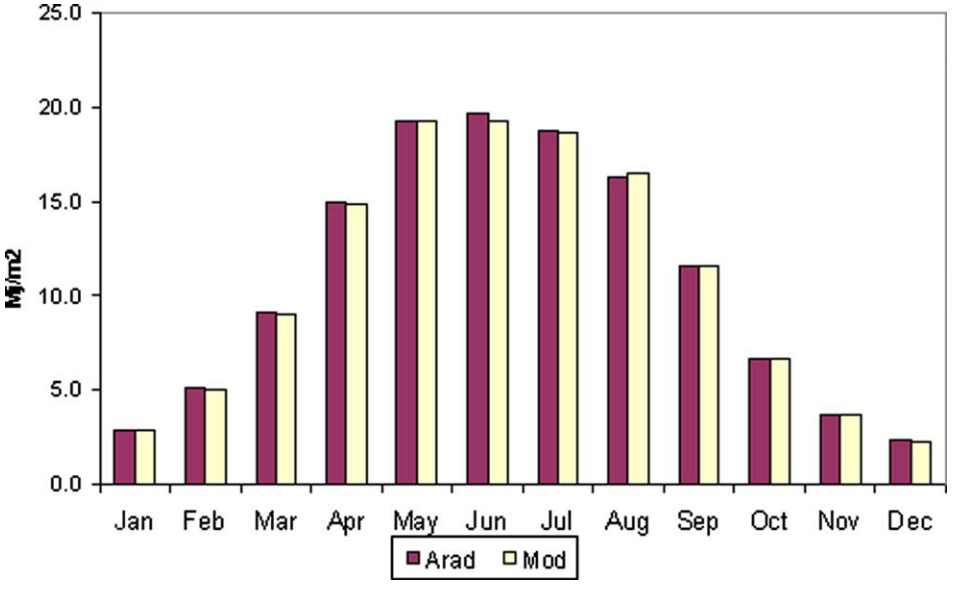

Figure 6. Comparison of mean daily radiation derived from sun hours from Rosslare and modelled radiation for an independent verification period of 1961–1970.

In recognition of the uncertainty associated with employing only one GCM or emissions scenario, ensemble mean scenarios of temperature, radiation and PE were produced sampling across all three GCMs and both the A2 (medium-high) and B2 (medium-low) emissions scenario were employed in the analysis. Ensembles or model

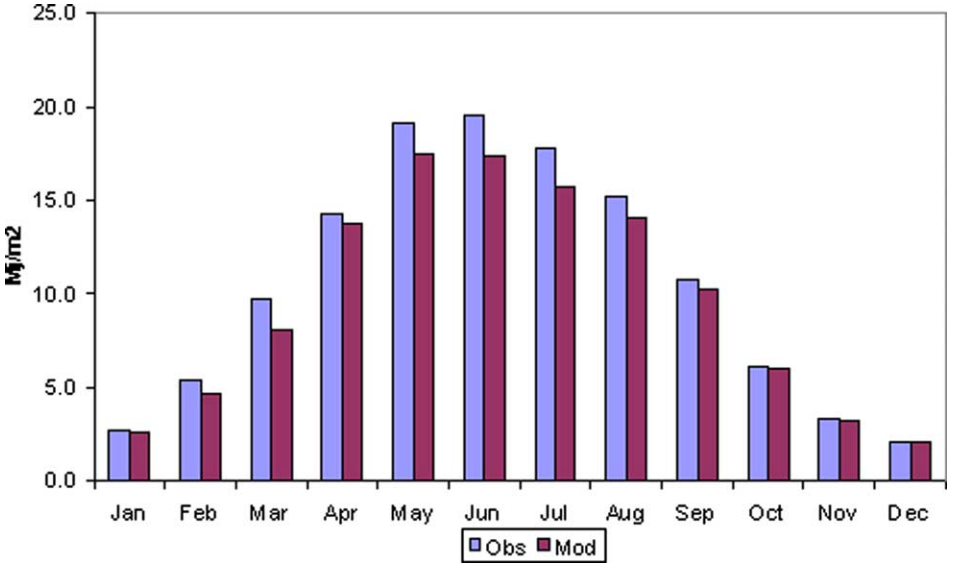

Figure 7. Comparison of observed mean daily radiation from Valentia and modelled radiation, calculated from sun hours employing the Angstrom formula, for an independent verification period of 1961–1970.

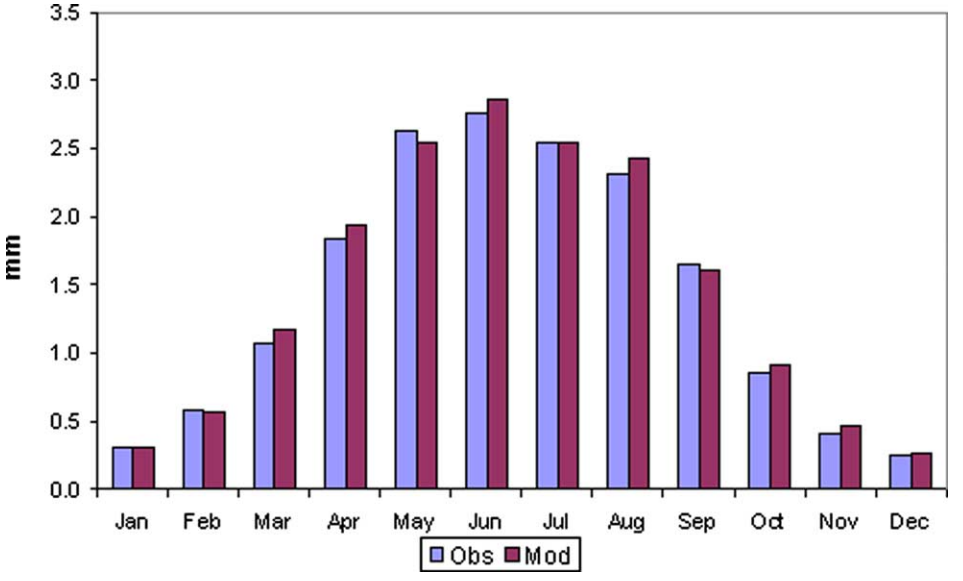

Figure 8. Comparison of calculated mean monthly potential evapotranspiration from Valentia and modelled potential evapotranspiration for an independent verification period of 1991–2000.

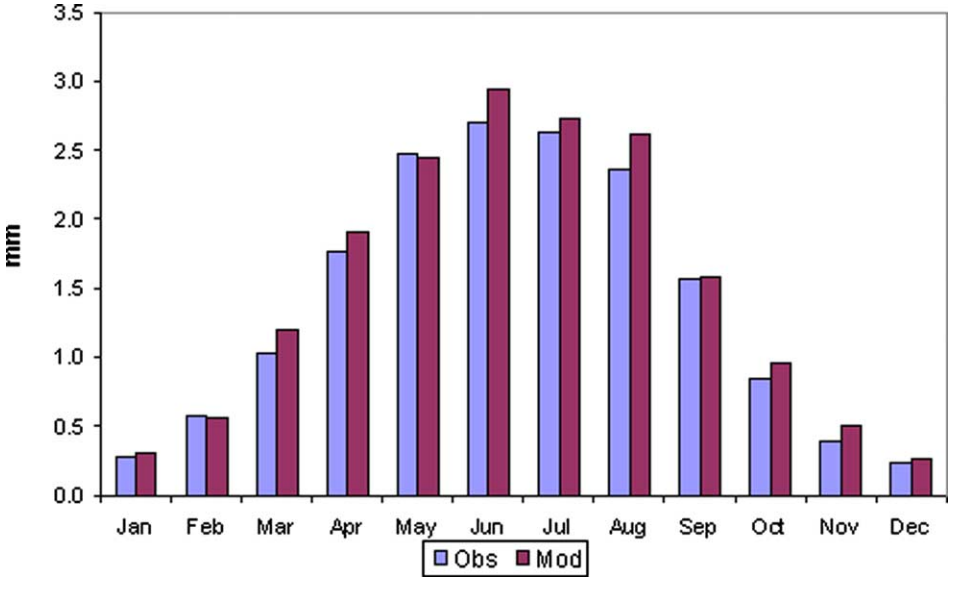

Figure 9. Comparison of calculated mean monthly potential evapotranspiration from Kilkenny and modelled potential evapotranspiration for an independent verification period of 1991–2000.

averages were calculated based on the Climate Prediction Index (CPI) (Murphy *et al.* 2004) which calculates a weighting factor for individual GCMs based on their ability to reproduce the statistics of the observed climate over a common time period. A modified version of the CPI was derived by Wilby and Harris (2006) for application to a narrower suite of GCM outputs and has been applied in an Irish context by Fealy and Sweeney (2007). Results are shown for three future time periods, the 2020s (2010–2039), the 2050s (2040–2069) and the 2080s (2070–2099). Thirty-year time periods are employed as standard in order to account for decadal and inter-decadal variability, which can be large for mid-latitude locations such as Ireland.

Temperature

The mean ensembles, produced from the CPI, suggest that by the 2020s average seasonal temperatures across Ireland will increase by between 0.75–1.0°C (Table 8) relative to the 1961–1990 'normal' period. A portion of this warming has already been experienced over the period since 1990. Results for the winter and autumn months display the largest inter-GCM difference (Figure 10), ranging from a marginal decrease to a +2°C increase in winter, while in autumn the range is +0.7°C to +1.8°C. By the 2050s, Irish temperatures are projected to increase by 1.4–1.8°C above the 1961–1990 period, with the greatest warming occurring during the autumn (Figure 10). While differences between the individual emissions scenarios are small for all seasons, the inter-GCM range is large, again indicating the requirement for output from multiple GCMs when conducting climate change research. Spatial differences also become more apparent during the 2050s, with an enhanced 'continental' effect becoming apparent (Figure 13).

This 'continental' effect becomes further enhanced by the 2080s period, particularly during the autumn season. This season accounts for the greatest warming for this period, with a mean increase of 2.7°C projected to occur (Figure 12). The mean temperature in all seasons is projected to increase by 2°C or more (Table 8). Ensemble mean summer temperatures are projected to increase by 2.5°C under the A2 emissions scenario, however, this increase may be as high as 3°C (Figure 12). Inter-model ranges again display a large range in the projections for the 2080s, particularly during the winter season.

Radiation

By the 2020s, ensemble mean seasonal radiation is projected to decrease in all but the summer months, which suggests no change relative to the 1961–1990 period (Figure

Table 8. Ensemble mean temperature increases for each season and time period.

Season	2020	2050	2080
DJF	0.7	1.4	2.1
MAM	0.8	1.4	2.0
JJA	0.7	1.5	2.4
SON	1.0	1.8	2.7

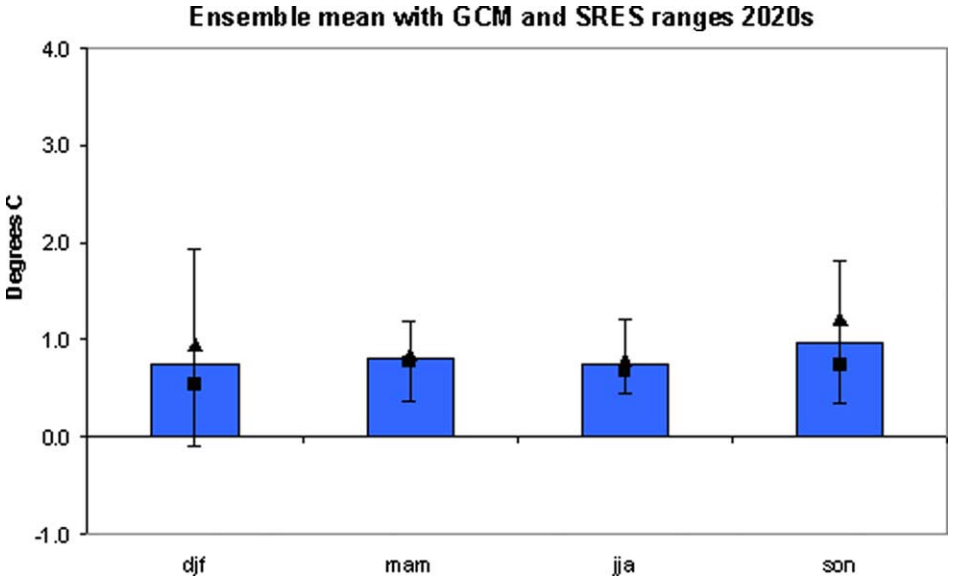

Figure 10. Ensemble mean temperature for the 2020s produced from the weighted ensemble of all GCMs and emissions scenarios (bars).
Note: Upper and lower ranges (lines) are the results from the individual GCMs and emissions scenarios. Ensemble A2 scenario (■) and B2 scenario (▲).

14). Individual results from the GCMs for the 2020s suggest a change in winter radiation of between +1 and –12%. An inconsistent signal is again apparent for spring, with individual GCM suggesting a range from a marginal, but positive increase of 0.5% to a decrease of 5%. For autumn, a more consistent signal of change is suggested, with all GCMs indicating a decrease in radiation.

By the 2050s, a greater seasonal divergence is apparent in radiation receipt, with the ensemble mean suggesting reductions of almost 11% during the winter months while an increase of 1.5% is projected to occur during the summer months (Figure 15). GCM ranges are also more consistent in projecting the direction of change, with the exception of the spring season, with one GCM suggesting a marginal increase in radiation receipt during this season.

These seasonal changes are further enhanced by the 2080s, with decreases of 13–18% being projected for the winter season by the individual emissions scenarios (Figure 16). The ensemble mean scenario projects a decrease of 16% in radiation for winter, while a small increase of 3% is projected to occur during the summer months. However, inter-GCM ranges are greatest for this season ranging from a decrease of 1.5% to an increase of 6% in receipts, by the 2080s.

Potential evapotranspiration

Due to the dependence of PE on radiation, projected changes in this variable are broadly in line with the changes projected in radiation for the future time periods (Figures 17–19) and are not discussed further for reasons of space.

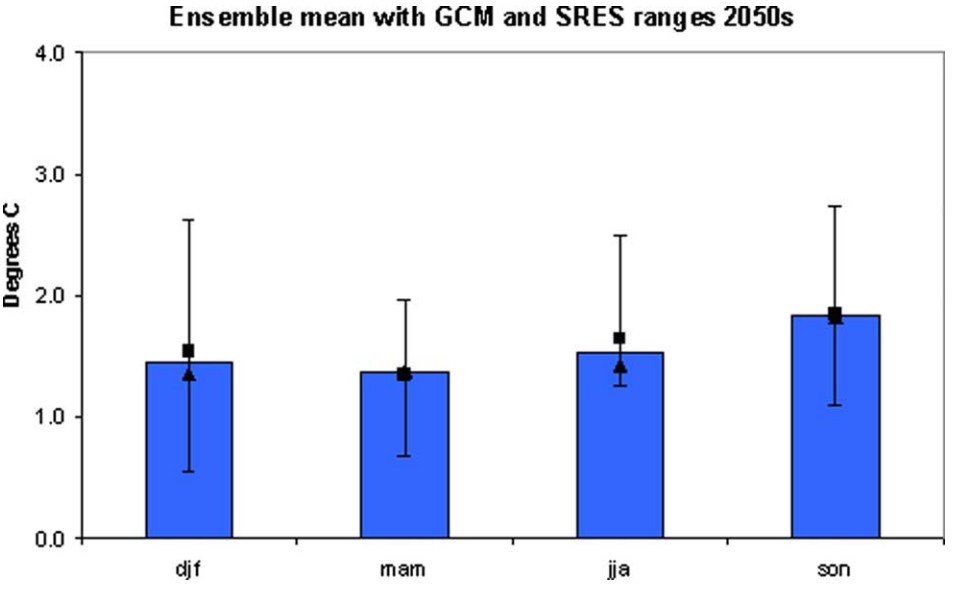

Figure 11. Ensemble mean temperature for the 2050s produced from the weighted ensemble of all GCMs and emissions scenarios (bars).
Note: Upper and lower ranges (lines) are the results from the individual GCMs and emissions scenarios. Ensemble A2 scenario (■) and B2 scenario (▲).

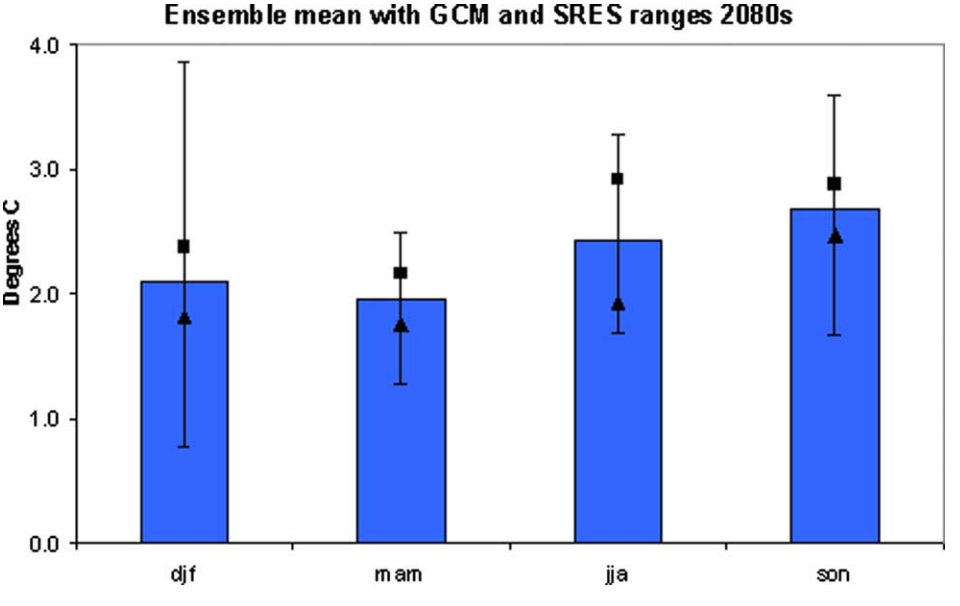

Figure 12. Ensemble mean temperature for the 2080s produced from the weighted ensemble of all GCMs and emissions scenarios (bars).
Note: Upper and lower ranges (lines) are the results from the individual GCMs and emissions scenarios. Ensemble A2 scenario (■) and B2 scenario (▲).

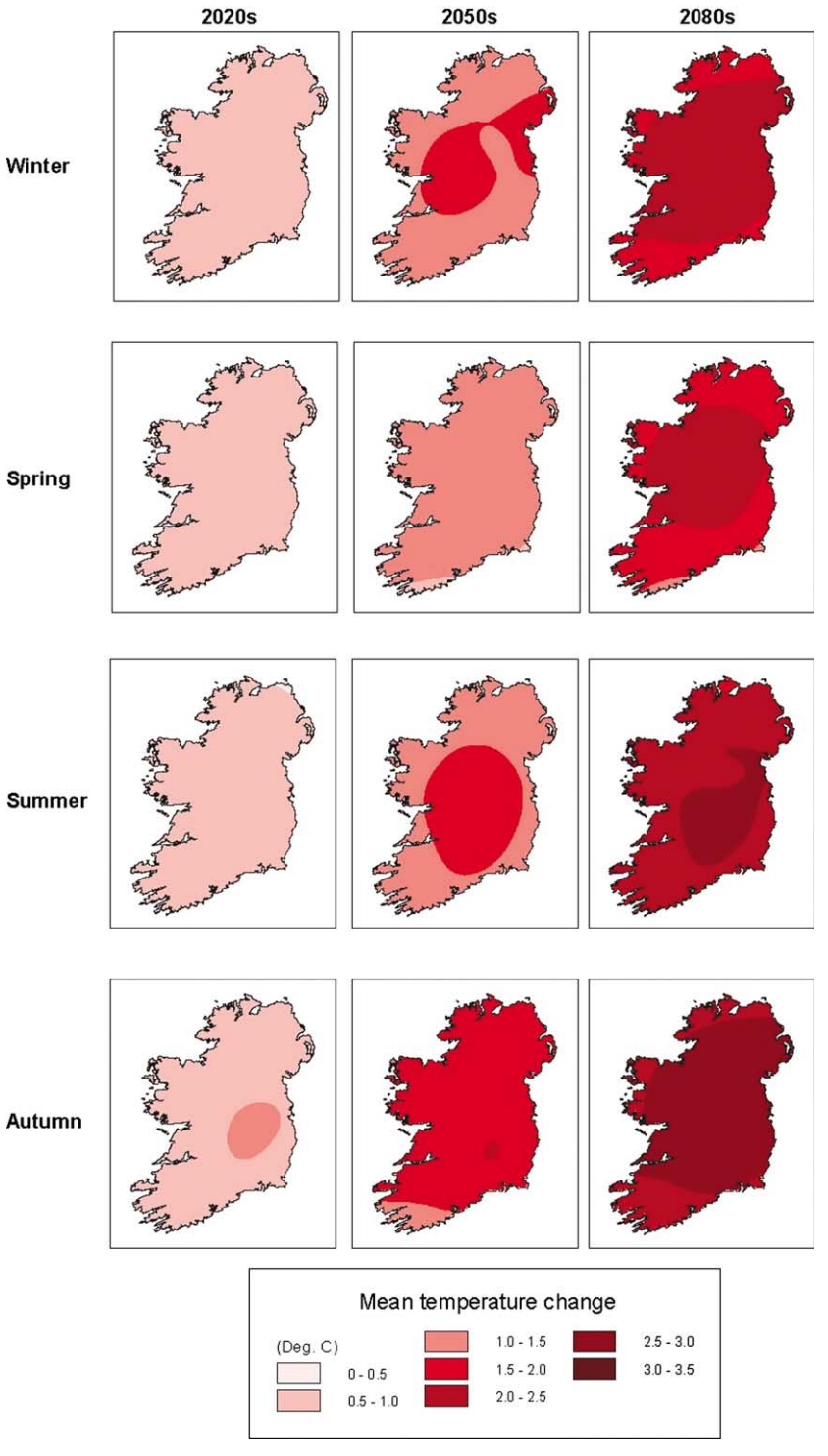

Figure 13. Ensemble mean seasonal temperature increase for the 2020s, 2050s and 2080s.

Projected future changes in extremes of temperature

Extreme climate events, such as the prolonged heat wave which occurred in Central Europe during the summer of 2003 or the severe flooding in Eastern Europe during the summer of 2002, tend to have a larger impact on human society than changes in the mean climate state. While Ireland has not experienced the type of extremes that have been witnessed in Central Europe, projected changes in the frequency and magnitude of extreme events are increasingly likely to have an effect on human activities in Ireland over the course of the present century. During the summer of 2006, much of Ireland suffered significant soil moisture deficits due to a combination of above average mean temperatures, which were more than 1°C higher than normal for the 1961–1990 period (nearly 2°C higher than normal for the 1961–1990 period in the midland stations of Clones and Kilkenny), and below average rainfall resulting in it being the warmest, driest and sunniest summer since 1995 (Met Éireann 2006). Poulter indices, which are derived from a combination of mean temperature, rainfall and sunshine and are a means of quantifying summer weather, calculated for the summer of 2006 recorded the third highest index value in a series that extends back for almost 100 years (Met Éireann 2006).

As temperature is a key meteorological parameter, changes in its frequency and magnitude are further, but provisionally, assessed to determine its likely impact as a consequence of projected climate change. Caution must be exercised with regard to any analysis of projected changes in extremes due to the uncertainties associated with regional projections of these events. In a recent analysis of climate extremes based on various downscaling methodologies, STARDEX (2006) found that performance of the models was better for temperature than precipitation, better for means than extremes, and best in winter and worst in summer. Additionally, the methodology employed in the current research was primarily focused on generating scenarios representing the projected mean climate state for the present century and therefore is likely to underestimate changes in the extremes of temperature. The results should therefore be interpreted as indicative of likely changes based on the projections of climate resulting from climate change.

Four core indices were selected for this analysis (Table 9). These indices are based on thresholds defined by percentiles rather than fixed values (STARDEX 2006), with the exception of Number of frost days, which requires minimum temperatures to be below 0°C. Figure 20 displays the station results for the four indices, on an annual basis, for the period 1961–2099, based on the modelled A2 ensemble data. Trends were found to be significant (0.01 significance level) at all stations and for all temperature indices employed in the analysis. The Hot-day threshold (tenth hottest day per year) indicates warming at all stations and is more pronounced at inland

Table 9. Indices of extremes employed in analysis.

Temperature indices of extremes	
Tmax 90th percentile	Hot-day threshold
Tmin 90th percentile	Cold-night threshold
Number of frost days	Frost days
Heat wave duration	Longest heat wave

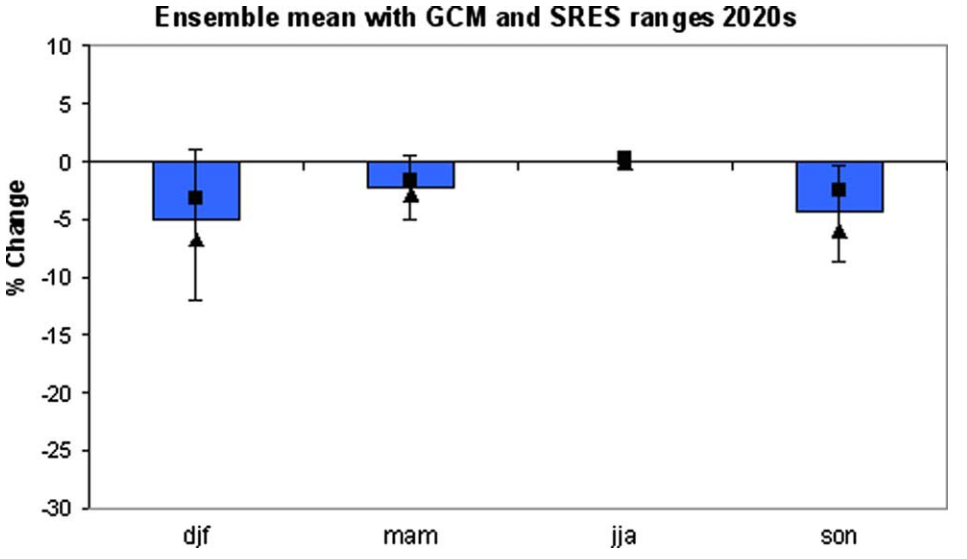

Figure 14. Ensemble radiation for the 2020s produced from the weighted ensemble of all GCMs and emissions scenarios (bars).
Note: Upper and lower ranges (lines) are the results from the individual GCMs and emissions scenarios. Ensemble A2 scenario (■) and B2 scenario (▲).

stations, away from the coast. Based on the modelled data, heat wave durations are also suggested to increase by up to 3–4 days per decade. A significant increase in cold night temperatures (tenth coldest night per year) is projected to occur and is

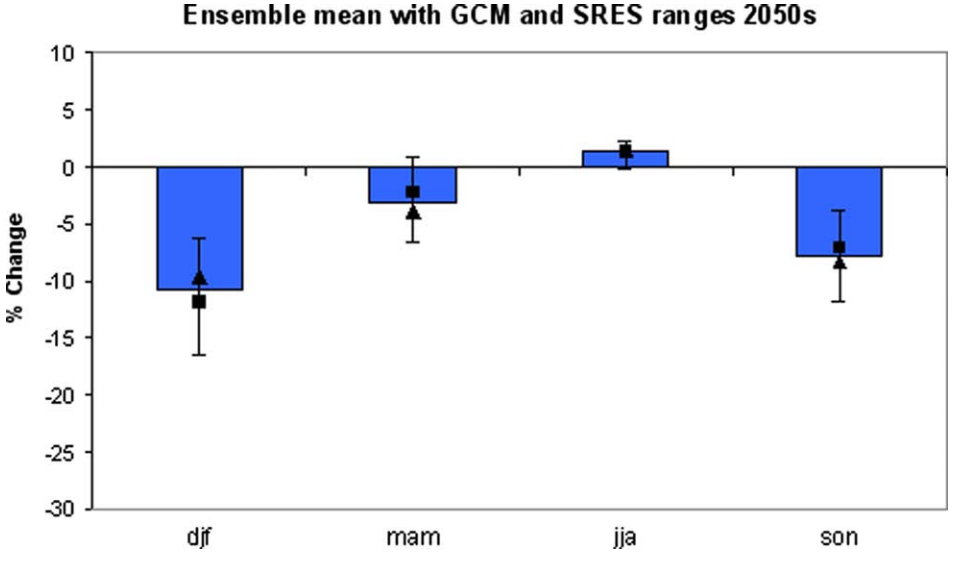

Figure 15. Ensemble radiation for the 2050s produced from the weighted ensemble of all GCMs and emissions scenarios (bars).
Note: Upper and lower ranges (lines) are the results from the individual GCMs and emissions scenarios. Ensemble A2 scenario (■) and B2 scenario (▲).

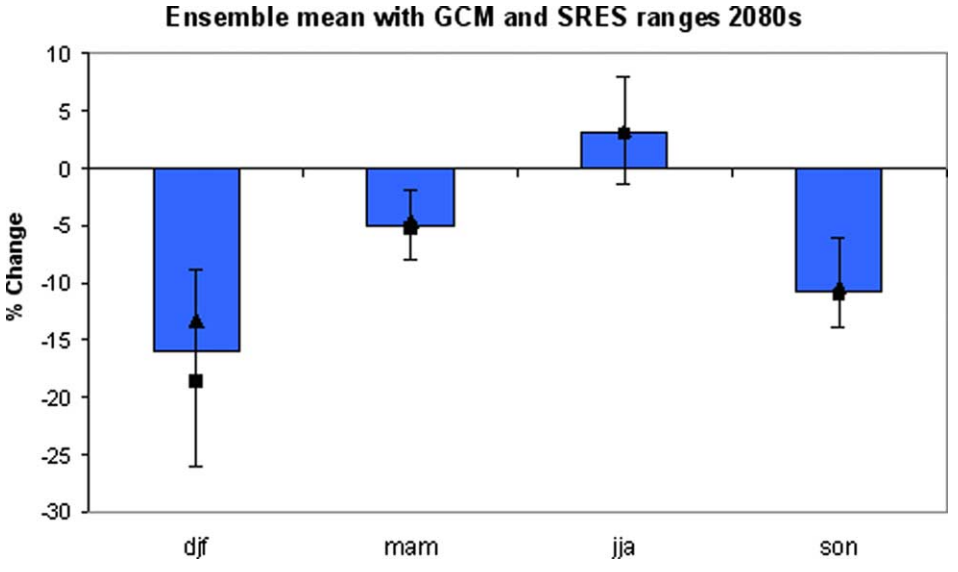

Figure 16. Ensemble radiation for the 2080s produced from the weighted ensemble of all GCMs and emissions scenarios (bars).
Note: Upper and lower ranges (lines) are the results from the individual GCMs and emissions scenarios. Ensemble A2 scenario (■) and B2 scenario (▲).

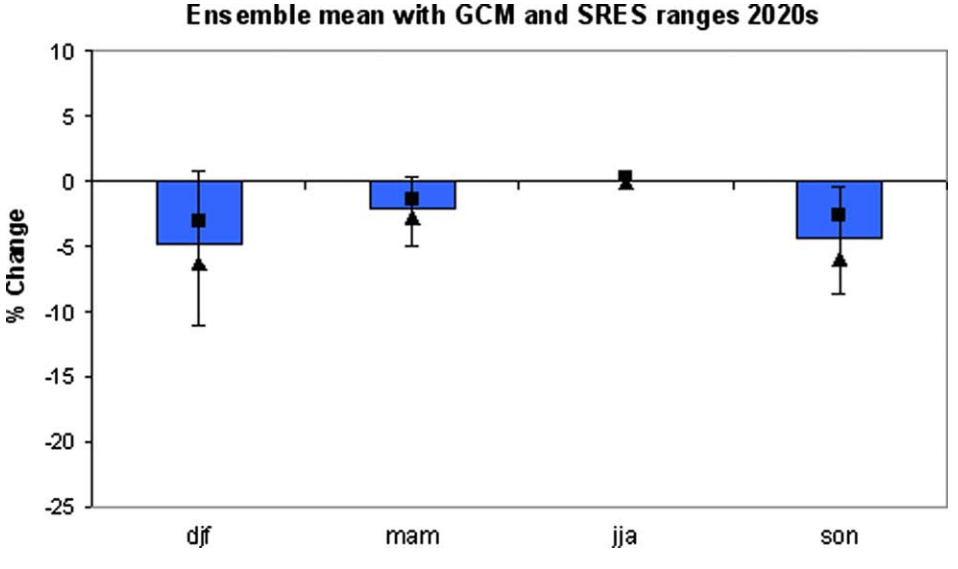

Figure 17. Ensemble PE for the 2020s produced from the weighted ensemble of all GCMs and emissions scenarios (bars).
Note: Upper and lower ranges (lines) are the results from the individual GCMs and emissions scenarios. Ensemble A2 scenario (■) and B2 scenario (▲).

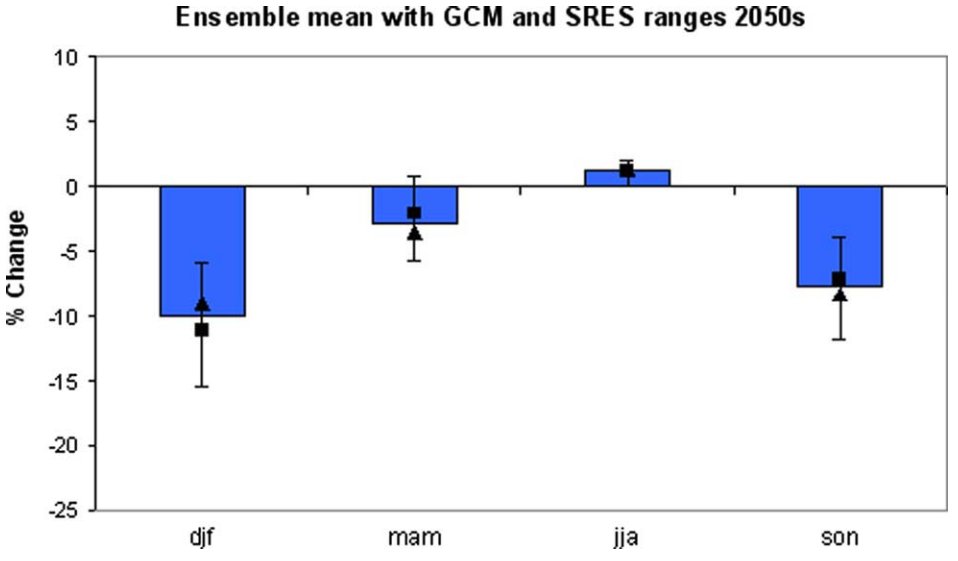

Figure 18. Ensemble PE for the 2050s produced from the weighted ensemble of all GCMs and emissions scenarios (bars).
Note: Upper and lower ranges (lines) are the results from the individual GCMs and emissions scenarios. Ensemble A2 scenario (■) and B2 scenario (▲).

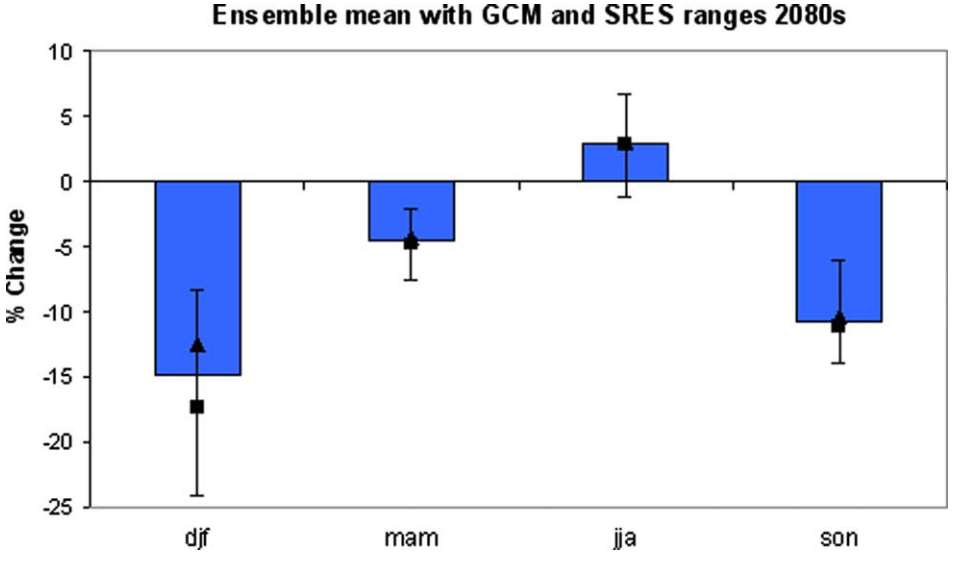

Figure 19. Ensemble PE for the 2080s produced from the weighted ensemble of all GCMs and emissions scenarios (bars).
Note: Upper and lower ranges (lines) are the results from the individual GCMs and emissions scenarios. Ensemble A2 scenario (■) and B2 scenario (▲).

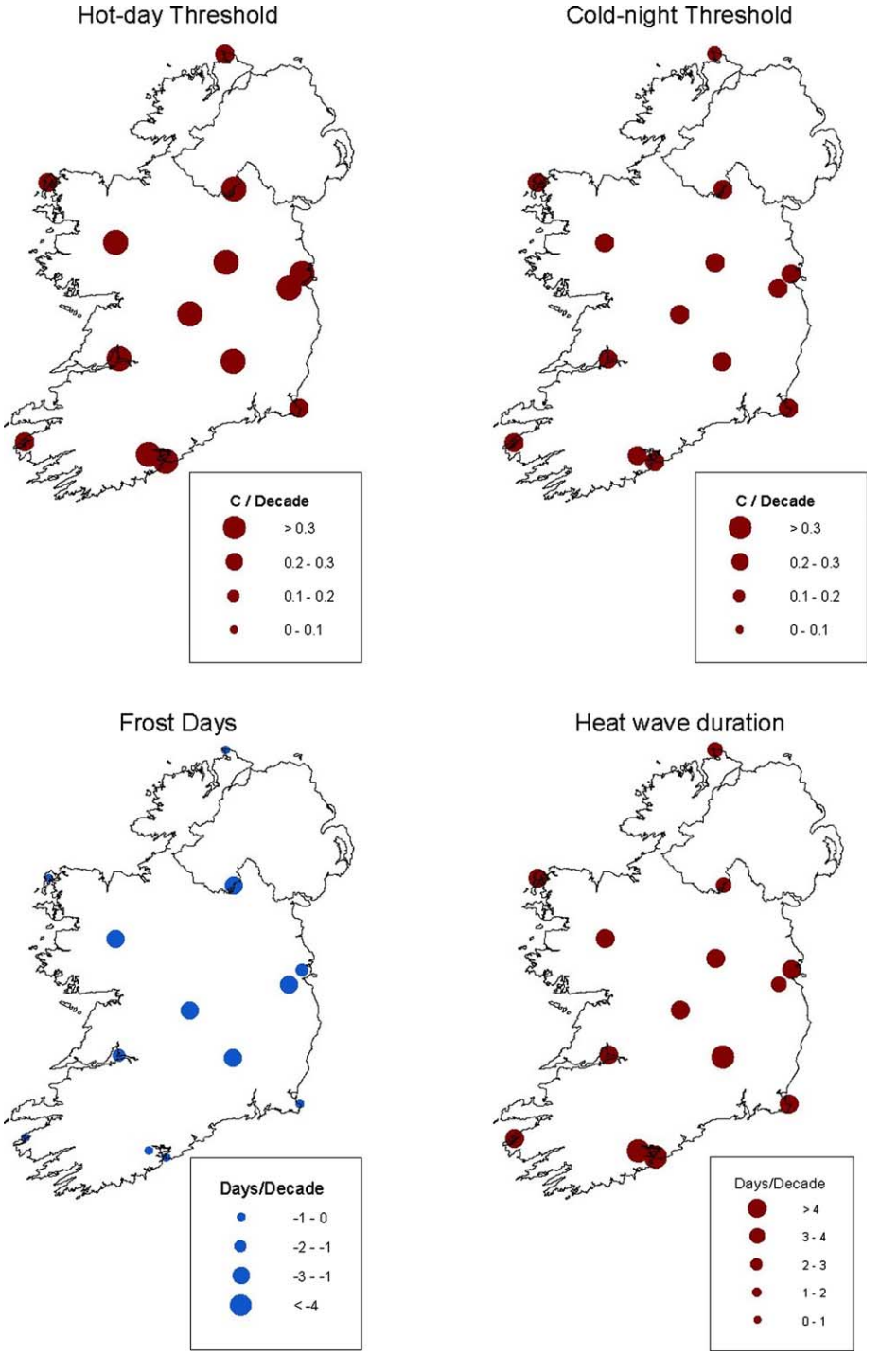

Figure 20. Trend/decade in the temperature indices for the A2 ensemble over the 1961–2099 period.
Note: All trends significant at 0.01 level.

probably associated with the projected and significant decrease in the number of frost days per decade.

While an assessment of these extreme indices on an annual basis is likely to mute the seasonal changes, all the temperature indices suggest significant trends that are consistent with observations and expectations of changes resulting from climate change. Over the 1961–2005 period, a significant increase in both maximum and minimum observed temperatures, resulting in fewer frost days and a shortening of the frost season, has been identified by McElwain and Sweeney (2007). The duration of heat waves was found to be increasing at a number of stations, while the number of consecutive cold days was found to be decreasing over this period.

While this section focused on changes in values at the 90^{th} percentile, suggested changes occurring above this cut-off are likely to have a smaller return period and be more extreme than experienced at present. Susceptibility to changes in the mean climate, but also to changes in extremes needs to adequately assessed in order to minimise potential future risks.

Conclusions

A number of studies have attempted to produce future climate scenarios for Ireland (McWilliams 1991, Sweeney and Fealy 2002, 2003a, 2003b) for use in impact studies to assess changes in agriculture, water resources, forestry, biodiversity and the marine environment (Sweeney *et al.* 2003; Holden *et al.* 2003, 2004; Charlton *et al.* 2006). However, these studies have acknowledged and inherent weaknesses due to the top-down and generally single trajectory approach of employing projections from just one GCM. While the single-trajectory approach has been common practice in the literature, quantification of uncertainties is becoming increasingly more important and feasible, primarily due to increased data availability from GCM modelling centres. To address this deficiency this paper presented a downscaling methodology for a selection of climate variables for Ireland that combined downscaled output from multiple GCMs. The methodology outlined, based on a stepwise multiple linear regression technique, can be readily applied where the predictand, or climate variable of interest, tends towards a normal or near normal distribution. An added advantage of this technique is that the error term of the regression equation can be employed to add a stochastic component to the resultant data series.

Having selected a parsimonious set of predictors from which to calibrate the seasonal transfer functions, which link the large-scale atmospheric predictors to the surface climate variable of interest, models were then assessed by comparing model output with observed data, for an independent verification period. Results from the independent verification period indicated that the seasonal models adequately captured the forcing component of the selected large- and local-scale atmospheric and surface predictors employed in the analysis. A comparable suite of predictors, from each of three GCMs, were then employed, in conjunction with the derived transfer functions, to produce the climate scenarios for each site, season and variable.

The seasonally and time averaged projections from the individual GCMs were found to vary both in direction and magnitude, largely reflecting uncertainties inherent in climate modelling arising from uncertainties associated with future emissions scenarios, GCM parameterisation, internal variations in the climate system and their representation, selection of initial forcing conditions for particular

GCM runs and the climate sensitivity of a model. In order to cater for some of these uncertainties in the present research, the CPI was employed to produce model averages or ensembles of the downscaled climate scenarios. While the method outlined in this paper takes into account uncertainties associated with the selected GCMs and emissions scenarios, no measure of the uncertainty due to the transfer functions is considered. This is an area that warrants further research.

The findings outlined in this paper reaffirm the importance of using an ensemble of GCMs and emissions scenarios in order to derive future projected changes in climate. In order to estimate how much confidence we can have in climate change projections and subsequent impact assessments, various sources of uncertainty need to be adequately accounted for.

Acknowledgements

The authors gratefully acknowledge the financial support provided by the Irish Environmental Protection Agency, as part of the Environmental Research Technological Development and Innovation (ERTDI) Programme 2000–2006. The authors would also like to thank Met Éireann for supplying the observational data.

Work undertaken on the diagnostics extremes indices software at King's College London and the Climatic Research Unit was funded by the Commission of the European Union under the STARDEX (http://www.cru.uea.ac.uk/projects/stardex) project (contract EUK2-CT-2001-00115). The European Climate Assessment project (http://www.knmi.nl/samenw/eca/) and US National Climatic Data Centre are thanked for the code, which forms the basis of this software.

The authors would also like to thank the anonymous reviewers and Dr Neil MacDonald for their helpful comments and suggestions on how to improve the paper.

References

Angstrom, A., 1924. Solar and terrestrial radiation. *Quarterly Journal of the Royal Meteorological Society*, 50, 121–126.

Brock, T.D., 1981. Calculating solar radiation for ecological studies. *Ecological Modelling*, 14, 1–19.

Busuioc, A., Von Storch, H., and Schnur, R., 1998. Verification of GCM-generated regional seasonal precipitation for current climate and of statistical downscaling estimates under changing climate conditions. *Journal of Climate*, 12, 258–272.

Charlton, R., *et al.*, 2006. Assessing the impact of climate change on water supply and flood hazard in Ireland using statistical downscaling and hydrological modelling techniques. *Climatic Change*, 74 (4), 75–492.

Fealy, R. and Sweeney, J., 2007. Statistical downscaling of precipitation for a selection of sites in Ireland employing a generalised linear modelling approach. *International Journal of Climatology*, 27, 2083–2094.

Holden, N.M., *et al.*, 2003. Possible change in Irish climate and its impact on barley and potato yields. *Agriculture and Forest Meteorology*, 116 (3–4), 181–196.

Holden, N.M., *et al.*, 2004. Climate change and Irish agriculture. *In*: T. Keane and J.F. Collins, eds. *Climate, weather and Irish agriculture, Joint Working Group on Agricultural Meteorology*. Dublin: Met Eireann, 359–382.

Hulme, M. and Carter, T.R. 1999. Representing uncertainty in climate change scenarios and impact studies. *In*: T. Carter, M. Hulme and D. Viner, eds. Representing uncertainty in climate change scenarios and impact studies, Proceedings ECLAT-2 Helsinki Workshop, 14–16 April, 1999. Norwich: Climatic Research Unit.

Huth, R., 2003. Sensitivity of local daily temperature change estimates to the selection of downscaling models and predictors. *Journal of Climate*, 17, 640–652.

IPCC, 2001. Climate change 2001: the scientific basis. *In*: J.T. Houghton, *et al.*, eds. *Contribution of Working Group I to the Third Assessment Report of the Intergovernmental Panel on Climate Change (IPCC)*. Cambridge: Cambridge University Press.

IPCC, 2007. Climate change 2007: the physical science basis of climate change. *In*: D. Qin and S. Solomon, eds. *Contribution of Working Group I to the Fourth Assessment Report of the Intergovernmental Panel on Climate Change*. Cambridge: Cambridge University Press.

Jones, P.D. and Moberg, A., 2003. Hemispheric and large-scale surface air temperature variations: an extensive revision and an update to 2001. *Journal of Climate*, 16, 206–223.

Jones, P., Hulme, M., and Briffa, K.R., 1993. A comparison of lamb circulation types with an objective classification scheme. *International Journal of Climatology*, 13, 655–663.

Jones, P.D. *et al.*, 2001. Global and hemispheric temperature anomalies – land and marine instrumental records. *In*: Carbon Dioxide Information Analysis Center, Oak Ridge National Laboratory, *Trends: a compendium of data on global change*. Oak Ridge, TN: US Department of Energy.

McElwain, L. and Sweeney, J., 2007. *Key indicators of climate change for Ireland*. Johnstown Castle, Wexford: Environmental Protection Agency.

McEntee, M., 1980. A revision of the equation relating sunshine hours to radiation income for Ireland. *Irish Journal of Agricultural Research*, 19, 119–125.

McWilliams, B.E., ed., 1991. *Climate change: studies on the implications for Ireland*. Dublin: Stationary Office.

Met ēireann, 2006. The weather of summer 2006. Available from: http://www.meteireann.ie/climate/monthly_summarys/summer06.pdf, Issued by the Climatology and Observations Division of Met Éireann, 1 September.

Murphy, J.M., *et al.*, 2004. Quantification of modelling uncertainties in a large ensemble of climate change simulations. *Nature*, 430, 68–772.

STARDEX , 2006. Downscaling climate extremes. Available from: http://www.cru.uea.ac.uk/projects/stardex/.

Sweeney, J. and Fealy, R., 2002. Future climate scenarios for Ireland using high resolution statistical downscaling techniques. *In*: F. Convery and J. Feehan, eds. *Achievement and challenge: Rio+10 and Ireland*. Dublin: Environmental Institute, University college Dublin, 172–178.

Sweeney, J. and Fealy, R., 2003a. Establishing reference climate scenarios for Ireland. *In*: J. Sweeney, *et al.*, eds. *Climate change scenarios and impacts for Ireland*. Johnstown Castle, Wexford: Environmental Protection Agency.

Sweeney, J. and Fealy, R., 2003b. A preliminary investigation of future climate scenarios for Ireland. *Biology and environment*. Special Issue *Proceedings of the Royal Irish Academy*, 102B, 3.

Sweeney, J., *et al.*, 2002. *Climate change: indicators for Ireland*. Johnstown Castle, Wexford: Environmental Protection Agency.

Sweeney, J., *et al.*, 2003. *Climate change: scenarios and impacts for Ireland*. Johnstown Castle, Wexford: Environmental Protection Agency.

Wigley, T.M.L., *et al.*, 1990. Obtaining sub-grid scale information from coarse-resolution general circulation model output. *Journal of Geophysical Research*, 95 (D2), 1943–1953.

Wilby, R.L. and Dawson, C.W., 2004. Using SDSM Version 3.1 – *A decision support tool for the assessment of regional climate change impacts*. User Manual.

Wilby, R.L. and Harris, I., 2006. A framework for assessing uncertainties in climate change impacts: low flow scenarios for the River Thames, UK. *Water Resources Research*, 42, W02419.1–W02419.10.

Wilby, R.L., *et al.*, 1998. Statistical downscaling of general circulation model output: a comparison of methods. *Water Resources Research*, 34, 2995–3008.

Wilby, R.L., Hay, L.E., and Leavesley, G.H., 1999. A comparison of downscaled and raw GCM output: implications for climate change scenarios in the San Juan River basin, Colorado. *Journal of Hydrology*, 225, 67–91.

Winkler, J.A., *et al.*, 1997. The simulation of daily temperature series from GCM output. Part II: Sensitivity analysis of an empirical transfer function methodology. *Journal of Climate*, 10, 2514–2532.

Yarnal, B., *et al.*, 2001. Developments and prospects in synoptic climatology. *International Journal of Climatology*, 21, 1923–1950.